PASJ: Publ. Astron. Soc. Japan , 1–??,

Dynamical friction on satellite galaxies

Michiko Fujii
Department of Astronomy, Graduate School of Science, the University of Tokyo, Tokyo, 113
fujii@astron.s.u-tokyo.ac.jp
Yoko Funato
General Systems Studies, Graduate Division of International and Interdisciplinary Studies, University of Tokyo, Tokyo, 153
funato@chianti.c.u-tokyo.ac.jp
and
Junichiro Makino
Department of Astronomy, Graduate School of Science, the University of Tokyo, Tokyo, 113
makino@astron.s.u-tokyo.ac.jp

(Received 2005 November 22; accepted 2006 May 1)

Abstract

For a rigid model satellite, Chandrasekhar's dynamical friction formula describes the orbital evolution quite accurately, when the Coulomb logarithm is chosen appropriately. However, it is not known if the orbital evolution of a real satellite with the internal degree of freedom can be described by the dynamical friction formula. We performed N-body simulation of the orbital evolution of a self-consistent satellite galaxy within a self-consistent parent galaxy. We found that the orbital decay of the simulated satellite is significantly faster than the estimate from the dynamical friction formula. The main cause of this discrepancy is that the stars stripped out of the satellite are still close to the satellite, and increase the drag force on the satellite through two mechanisms. One is the direct drag force from particles in the trailing tidal arm, a non-axisymmetric force that slows the satellite down. The other is the indirect effect that is caused by the particles remaining close to the satellite after escape. The force from them enhances the wake caused in the parent galaxy by dynamical friction, and this larger wake in turn slows the satellite down more than expected from the contribution of its bound mass. We found these two have comparable effects, and the combined effect can be as large as 20% of the total drag force on the satellite.

Key words: galaxies: evolution — galaxies: interactions — galaxies: kinematics and dynamics — methods: numerical — stellar dynamics

1. INTRODUCTION

The evolution of satellite galaxies has been studied by a number of researchers both theoretically and using numerical simulations. However, even though it is a basic and simple problem, our understanding is still rather limited.

Using N-body simulation of a rigid satellite within an N-body model of the parent galaxy, van den Bosch et al. (1999) found that the orbital eccentricity of a satellite galaxy tends to be roughly constant. Previous theoretical studies based on Chandrasekhar's dynamical friction formula (Chandrasekhar 1943) predicted circularization of the orbit. Thus, there was rather serious qualitative difference between the simulation result and the theoretical model.

In N-body calculations of van den Bosch et al. (1999), the parent galaxy was modeled as an N-body system, while the satellite was treated as one massive softened particle. Thus, the tidal mass loss was ignored in their calculation. Jiang and Binney (2000) performed a self-consistent N-body simulation of the evolution of a satellite galaxy, in which both the satellite and the parent galaxy were treated as N-body system. They compared the result with that of a semianalytical model, in which the orbit of the satellite evolved through the dynamical friction expressed by Chandrasekhar's formula. The agreement between the simulation and semianalytic model was not good. Velazquez & White (1999) performed similar comparison, and found that it was possible to make simulation result and semianalytic model agree to each other, if they use the Coulomb logarithm as a fitting parameter. Taylor & Babul (2001) constructed a more sophisticated model for the evolution of the satellite, and demonstrated that it could reproduce the simulation results of Velazquez & White (1999) quite accurately.

The dynamical friction formula is given by

$$\frac{d\boldsymbol{v}_{\rm s}}{dt} = -16\pi^2 G^2 m(M_{\rm s}+m)\log\Lambda \frac{\int_0^{v_{\rm s}} f(v_{\rm m}) v_{\rm m}^2 dv_{\rm m}}{|\boldsymbol{v}_{\rm s}|^3}\boldsymbol{v}_{\rm s}. \quad (1)$$

Here, $v_{\rm s}$ is the velocity of the satellite, G is the gravitational constant, $M_{\rm s}$ and m are the masses of the satellite galaxy and field particles of the parent galaxy, and $f(v)$ is the distribution function of field particles at the position of the satellite. We assumed that the velocity distribution is isotropic, which is true at least for the initial model of the parent galaxy we consider in this paper. The term

$\log\Lambda$ is the Coulomb logarithm given by

$$\log\Lambda = \log\left(\frac{b_{\max}}{b_{\min}}\right). \quad (2)$$

Here, $b_{\max}$ and $b_{\min}$ are the maximum and the minimum impact parameters for gravitational encounters between the satellite galaxy and the field stars in the parent galaxy. For the lower cutoff, it is natural to set $b_{\min}$ to the order of the virial radius of the satellite galaxy (White 1976). For the upper cutoff, in many studies the size of the parent galaxy R has been used (e.g., Murai & Fujimoto 1980; Helmi et al. 1999; Johnston et al. 1995). Jiang and Binney (2000) followed this tradition and used $\log\Lambda = 8.5$, while Velazquez & White (1999) varied it to obtain the best agreement, and the value they used was $1 \sim 2$. Clearly, however, one cannot use the Coulomb logarithm as a fitting parameter, since its value should be determined from the mass distributions of the satellite and the parent galaxy.

Hashimoto et al. (2003, hereafter H03) showed that Chandrasekhar's dynamical friction formula does give the result which is consistent with the simulation result, when the integration over the impact parameter is carried out correctly. Equation (2) was obtained assuming that the distribution of the field stars is uniform and infinite. We need to apply the upper cutoff since the integration would diverge without the cutoff. However, the actual N-body system has a finite size so that the integration over the mass distribution could not diverge. They pointed out that, if this integration over the mass distribution of the parent galaxy is correctly performed, the discrepancy between N-body simulation result and the model with analytic estimate disappears. The exact integration over all encounters generally resulted in the Coulomb logarithm smaller than the value given by equation (2) with $b_{\max} = R$, simply because the density drops off at large radii. The use of equation (2) with $b_{\max} = R$ is the same as to assume that the parent galaxy is a sphere of radius R with a constant density same as the local density around the satellite. Also, it implies that the orbit of the satellite is a straight line. However, since the density drops off and the orbit of the satellite is not a straight line, the actual dynamical friction is smaller. If we set the cutoff radius as the distance of the satellite from the center of the parent galaxy, equation (1) gives the result in good agreement with the N-body simulation.

H03 resolved the discrepancy between the theoretical and numerical results for the case of a rigid satellite. The formula they proposed, and a modified version of it (Zentner & Bullock 2003) are used in recent studies of the evolution of subhalos and satellite galaxies. In such studies, a self consistent N-body model is used for the satellite (or subhalo) and its orbit is integrated numerically using the dynamical friction formula, to express the time variation of the tidal field. This technique has been used by a number of researchers (Bullock & Johnston 2005; Johnston et al. 1995; Ibata & Lewis 1998; Portegies Zwart et al. 2004).

However, there is no guarantee that the orbital evolution of a live satellite is correctly described by the dynamical friction formula of H03. The results of previous studies (Jiang and Binney 2000; Velazquez & White 1999) suggest that the disagreement between simulation and semianalytic model with dynamical friction formula is due to the incorrect choice of the Coulomb logarithm. Even so, there has been no study in which the dynamical friction formula of H03 was directly compared to a fully self-consistent N-body simulation. That means the results can be very different.

In this paper, we performed such a direct comparison between fully self-consistent N-body simulation and semianalytic model. We found a serious disagreement, and we investigated the reason of that disagreement. Our main findings can be summarized as follows. The disagreement does exist, but in the direction opposite to that observed in previous studies. The orbital decay in the N-body simulation was significantly faster than that in the semianalytic model with the dynamical friction formula of H03. We investigated the cause of this disagreement, and found that the main causes are the effect of particles which are stripped from the main body of the satellite by the tidal field of the parent galaxy. These escaped particles exert drag forces to the main body of the satellite in two different ways. The first one is the direct gravitational force. Since the distribution of the escaped particles is not axisymmetric around the center of the parent galaxy, their gravity can change the orbital energy of the satellite, and it turned out that the forces integrated over all escaped particles effectively works as a drag force. The second one is the enhancement of the dynamical friction. Escaped particles typically go away from the satellite rather slowly. In other words, they move together with the satellite for a rather long time. Thus, from the point of view of the field particles, these "escaped" particles are still effectively part of the satellite, since the gravitational force they feel is the combined effect of the main body of the satellite and "escaped" particles which still are close to it. The dynamical friction on the body of the satellite is therefore bigger than what would be there if there are no such escaped particles. We found that these two effects have comparable strength and the combined effect explains the disagreement between the N-body simulation and semianalytic calculation.

This paper is organized as follows. In section 2 we describe the simulation method and initial conditions. In section 3 we give the result. The semianalytic model gave the orbital decay significantly slower than that observed in the N-body simulation. In section 4 we discuss the cause of this discrepancy. Section 5 is for a summary and discussions.

2. Numerical methods

2.1. Initial condition

We consider a simple problem of one spherical satellite galaxy orbiting in a spherical parent galaxy. This is essentially the same problem as that studied by H03. In the following we describe the initial model.

We adopted a King model with non-dimensional central potential $W_0 = 9$ as the model of the parent galactic halo and $W_0 = 7$ as that of the satellite halo. The system of units is the Heggie unit (Heggie & Mathieu 1986), where the gravitational constant G is 1 and the mass and the binding energy of the parent galaxy are 1 and 0.25, respectively. Initially, the satellite is placed at distance 1.5 from the center of the parent galaxy, with the velocity of 0.45. Assuming that the parent galaxy represents our Galaxy with total mass $M = 10^{12} M_\odot$ and the circular velocity $V_c = 250$ km s^{-1}, the initial distance and velocity of the satellite galaxy are 60 kpc and 140 km s^{-1}. Unit time in the Heggie unit corresponds to 130 Myr.

In table 1, we summarize the model parameters and initial conditions of our N-body simulations. Most of the parameters are the same as those used in H03. We chose the initial velocity slightly larger than what is used in H03, to keep the mass loss rate smaller. This choice allowed us to follow the evolution of satellite for more than 10 orbits.

2.2. N-Body Simulation

In the N-body simulation, both the parent galaxy and the satellite were expressed as self-consistent N-body models. The number of particles N of the parent is 10^6 and that of the satellite is 5×10^4. The number of particles in the satellite should be large enough that the relaxation effect does not seriously affect the mass loss from the satellite. Since the initial half-mass relaxation time of the satellite is about 160 in our system of units, relaxation effect is small.

The number of particles in the parent galaxy should be determined so that the two-body relaxation effect on particles in the parent galaxies and that in satellite galaxies are small compared to the velocity dispersion of particles. Since the velocity dispersion of particles in the parent galaxy is much higher than the internal velocity dispersion of satellite particles, we only need to consider the heating of satellite particles due to encounters with particles in the parent galaxy. The timescale of this heating, T_h, is expressed as

$$T_h = t_{rh,p} \frac{\sigma_s^2}{\sigma_p^2}, \tag{3}$$

for the first-order approximation, where $t_{rh,p}$ is the half-mass relaxation timescale of the parent galaxy, σ_s and σ_p are the velocity dispersions of the satellite and the parent galaxy, respectively. For our choice of initial model and number of particles, $T_h \sim 10^3$ and it is sufficiently longer than the duration of the simulation.

We used a Barnes-Hut treecode (Barnes & Hut 1986; Makino 2004) on GRAPE-6A (Fukushige et al. 2005). We used opening angle $\theta = 0.75$ with center-of-mass (dipole-accurate) approximation. The maximum group size for GRAPE calculation (Makino 1991) is 8192. For the time integration a leapfrog integrator with a fixed stepsize of $\Delta t = 1/256$ is used. The potential is softened using the usual Plummer softening, with the softening length $\epsilon = 0.00625$. This same softening is used for all interactions. The total energy was conserved to be lower than 0.02 % throughout the simulation.

Table 1. Model Parameters of N-body Simulations

Parameters	Parent	Satellite
Galactic halo	King 9	King 7
Total mass	1.0	0.01
Binding energy	0.25	0.25×10^{-3}
Half-mass radius	0.98	0.081
N	10^6	5×10^4
Initial position		(1.5, 0, 0)
Initial velocity		(0, 0.45, 0)

To calculate the mass and orbit of the satellite, we need to identify the particles which belong to the satellite. We determine these particles by an iterative procedure (Funato et al. 1993). One particle belongs to the satellite if its binding energy to the satellite is negative. Potential energy is calculated using all other particles which belong to the satellite, and kinetic energy is calculated relative to the center-of-mass motion of the satellite.

2.3. Semianalytic Integration

We performed semianalytic calculations to follow the evolution of the satellite orbits. Our procedure is the same as that used in H03. The satellite is modeled as a single particle with variable mass and size, and the parent as a fixed gravitational potential. The potential of the parent is a King model with $W_0 = 9$ which has the same mass and scale as that used in the N-body simulation.

For the dynamical friction, we used the standard dynamical friction formula of equation (1). We adopted the following form proposed by H03

$$\log \Lambda = \log \left(\frac{R_s}{1.4 \epsilon_s} \right), \tag{4}$$

for the Coulomb logarithm, where R_s is the distance between the center of the parent galaxy and the satellite galaxy and ϵ_s is the virial radius of the satellite.

In equations (1) and (4), we use the self-bound mass and virial radius of the satellite galaxy as M_s and ϵ_s. For these quantities, we used the values obtained in N-body simulations.

3. Simulation Result

Figure 1 shows nine snapshots of the satellite galaxy projected onto the x-y plane. Initially, the satellite is located at distance 1.5 from the center of the parent galaxy. At $T = 3$, it is close to the first pericenter passage. Due to the strong tidal field of the parent galaxy, the satellite becomes elongated. At $T = 9$, particles stripped inward and outward form clear tidal arms, and the leading arm starts to form a circular ring. As time proceeds, more and more mass is stripped out and at the same time the orbit of the satellite shrinks. At $T = 24$, stripped particles form complex collection of rings and spiral patterns.

Figure 2 shows the evolution of the bound mass of the satellite. At each pericenter passage, a significant amount

of mass is lost. After the pericenter passage at around $T = 45$, the satellite is disrupted.

Figure 3 shows the orbital evolution of the satellite obtained by the N-body simulation. We also showed the result of semianalytic calculations. The dashed curve shows the semianalytic calculation in which the mass and the size of the satellite were changed using the result of N-body simulation. The dotted curve showed the semianalytic calculation in which the mass and size of the satellite were kept unchanged from their initial values.

Even though we adopted the prescription for Coulomb logarithm proposed by H03, the agreement between the N-body simulation result and the result of semianalytic orbit integration (dashed curve) is rather poor. After the first pericenter passage, the decrease of the apocenter distance is smaller by about a factor of two for the semianalytic integration. This factor-of-two difference continues to exist for entire simulation period. In fact, the N-body simulation result is closer to the other semianalytic curve, for which we ignored the change of the mass (and the size) of the satellite, at least for the first several orbits. Thus, taking into account the change of the mass of the satellite somehow makes the agreement between the N-body simulation and semianalytic calculation worse. Dynamical friction formula, based on the instantaneous mass and size of the satellite, significantly underestimates the actual drag force on the satellite.

This result is quite different from the results of previous studies. Jiang and Binney (2000) performed similar comparison between an N-body simulation and a semianalytic calculation, and their result was that the semianalytic calculation resulted in faster orbital evolution. They used constant $\log\Lambda$ and this must be the cause of the difference. We used distance-dependent $\log\Lambda$ of H03, and we found that the result is over-corrected. The semianalytic model resulted in the orbital evolution much slower than the result of the N-body simulation.

We have performed many simulations with different initial orbits and initial satellite model, but for all cases the result is similar. When mass loss from the satellite is significant, the semianalytic model of H03 failed to reproduce the orbit.

4. Interaction between escaped particles and the satellite

Since the difference between the H03 model and our N-body simulation is that we used self-consistent model for the satellite, the cause of the discrepancy must be the interaction between the orbital motion of the satellite and its internal degree of freedom. There are several ways through which the internal degree of freedom of the satellite effectively operate as the drag force to its orbital motion. For example, a satellite is dynamically heated by "bulge shock" (Spitzer 1987) at each pericenter passage. The energy used to heat the internal motion of the satellite must have come from the orbital motion.

However, the internal energy of the satellite is much smaller than the orbital energy and not enough to explain the orbital evolution. In the following, we consider two mechanisms which are potentially more efficient than simple heating of internal motion.

The first mechanism is the interaction between the escaped particles and the satellite. In figure 1, particles escaped outward form rather impressive trailing spiral arms, while particles escaped inward form a ring-like structure. This means the gravitational interaction between the escaped particles and the main body of the satellite is not symmetric. To the trailing spiral arm, the satellite exerts some tidal torque, since the angular velocity of the satellite is faster than that of the arm. On the other hand, the ring would not exert much torque to the satellite, since it is axisymmetric. This mechanism is essentially the same as the effect of non-conserving mass transfer from a binary of two stars. The gas escaped from the L_2 point acquires the angular momentum through the interaction with the orbital motion of the binary, resulting in the loss of the orbital angular momentum of the binary. In this paper we call this effect the direct interaction between the escaped stars and the satellite.

The second one is what we named "indirect interaction". Many of the particles which are stripped out of the satellite remain close to the satellite. This is part of the reason why the direct interaction can be important. If escapers quickly go away from the satellite, the loss of the energy and angular momentum due to the tidal torque would be small.

If some of the escapers remain close to the satellite, they might result in the enhancement of dynamical friction. One way to understand dynamical friction is to regard it as the gravitational pull by the wake of particles generated by the satellite galaxy. The strength of the wake depends on the mass which generates the wake. If some escaped particles remain close to the satellite, they help making the wake, resulting in the enhancement of the dynamical friction.

In the following two sections, we evaluate quantitatively these two effects in turn.

4.1. Direct interaction with escapers

Here, we measure the effect of the direct interaction. The acceleration (or deceleration) of the satellite by the interaction with the escaped particle is defined simply as

$$\boldsymbol{a}_{\rm di} = \frac{1}{M_{\rm s}} \sum^{i} \sum^{j} \boldsymbol{f}_{ij}, \tag{5}$$

where the summation for i is taken for particles which escaped from the satellite, and summation over j is for particles which are bound to the satellite. The force $\boldsymbol{f}_{ij}$ is the gravitational force from particle i to particle j.

We calculate change in the specific orbital energy by this direct interaction as

$$\Delta E_{\rm di} = \int_0^T \boldsymbol{a}_{\rm di} \cdot \boldsymbol{V} dt, \tag{6}$$

where $\boldsymbol{V}$ is the center-of-mass velocity of the satellite. Both $\boldsymbol{a}_{\rm di}$ and $\boldsymbol{V}$ are calculated from simulation result.

Figure 4 shows the direction and strength of $\boldsymbol{a}_{\rm di}$ along with the orbit of the satellite. For this figure, we separate $\boldsymbol{a}_{\rm di}$ into the contribution of escaped particles with the distance from the center of the galaxy larger than that of satellite (outward escapers, $\boldsymbol{a}_{\rm out}$) and the rest (inward escapers, $\boldsymbol{a}_{\rm in}$). By definition, $\boldsymbol{a}_{\rm out}$ points outwards and $\boldsymbol{a}_{\rm in}$ inwards. If we compare the direction of these two terms and the orbit of satellite, we can see that the gravitational force from outward escapers generally acts as the drag force, while that from inward escapers changes the direction rather often. For example, around the time of the first pericenter passage (after $T=3$), the inward term clearly points to the direction of motion, but it quickly changes the direction and works as the drag, until the satellite reaches the apocenter. The outward term generally works as the drag force, even when the satellite is going outward.

Figure 5 shows the change of the orbital binding energy of the satellite due to these forces from escaped particles. We can see that the contribution of outward escapers works as the drag, and that from inward escapers have the opposite effect. The total effect is the drag. For the outward contribution, the force and resulting energy change comes mainly from the particles which form "trailing arm", and that is the reason why it acts as the drag force for most of time.

Figure 6 shows the time change of $\Delta E_{\rm di}$. For comparison, we also show the energy change due to dynamical friction $\Delta E_{\rm df}$ calculated using equation (1) and the specific total energy change $\Delta E_{\rm total}$ obtained from N-body simulation.Here, $\Delta E_{\rm total}$ is defined as

$$\Delta E_{\rm total} = \int_0^T (\boldsymbol{a}_{\rm s} - \boldsymbol{a}_{\rm p}) \cdot \boldsymbol{V} dt, \tag{7}$$

where $\boldsymbol{a}_{\rm s}$ is the center-of-mass acceleration of the satellite, $\boldsymbol{a}_{\rm p}$ is the acceleration due to the potential of the parent galaxy, which is estimated as

$$\boldsymbol{a}_{\rm p} = -\frac{GM(r)}{r^3}\boldsymbol{r}, \tag{8}$$

where r is the distance from the center of mass of the parent to that of the satellite and $M(r)$ is the mass of the parent within r. We calculated $M(r)$ from the density profile of the King model with $W_0 = 9$, which is the initial model of the parent halo in our N-body simulations.

To calculate $\Delta E_{\rm total}$, we assumed that the distribution of stars within the parent galaxy is unchanged, even though the satellite transfers part of its mass and orbital energy. Since the mass of the satellite is a small fraction of the total mass of the parent galaxy, the change of the structure of the parent galaxy is small, and our treatment should give fairly accurate estimate of the energy change of the satellite.

From figure 6 we can see that the dynamical friction of H03 formula accounts for about 80% of the total deceleration, and that the direct interaction accounts for about half of the remaining 20% of the deceleration. Thus, we can conclude that the direct interaction is significant, but other effects are not negligible. In the next section we analyze the indirect contribution of escaped particles.

4.2. Enhancement of the dynamical friction

Particles which have been stripped out of the satellite but still are close to it can increase the dynamical friction to the satellite. As far as these "escaped" particles move together with the satellite, the center-of-mass motion of these escaped particles and the satellite feels the dynamical friction, and the strength of the dynamical friction is determined by the total mass including the escaped particles. A practical problem with this view is that it is not easy to quantitatively evaluate the strength of the dynamical friction on the bound part of the satellite galaxy. If the mass distribution of the satellite and the escaped particles at a given time is known, we can calculate the dynamical friction on the center-of-mass motion of them by evaluating the linear momentum change of field particles. However, to calculate the drag force on the bound part is a bit complicated, since we need to evaluate the drag force from the perturbed distribution of field stars back to the satellite.

In the following, we give a simple model to calculate this effect. First, let us consider the simplest case, in which two softened point-mass objects move in a uniform distribution of field particles. Figure 7 shows the configuration we consider. Two massive objects, S_1 and S_2, with equal masses M, move along z axis with velocity V_0. To simplify the calculation, let us consider the case that field particles are at rest and distributed uniformly and isotropically. We calculate the enhancement of dynamical friction acting on S_1 as a function of the distance between S_1 and S_2 in the following way.

The acceleration of S_1 due to dynamical friction is given by

$$\frac{d\boldsymbol{v}_1}{dt} = n\boldsymbol{V}_0 \int_0^{b_{\rm max}} \int_0^{2\pi} \Delta\boldsymbol{V}_{1\parallel}\ b_1\ d\theta_1\ db_1, \tag{9}$$

where n is the number density of the field particles, $\boldsymbol{V}_0$ is the initial velocity vector of S_1, $\Delta\boldsymbol{V}_1$ is the change in velocity of S_1 caused by one encounter with a background particle, $\Delta\boldsymbol{V}_{1\parallel}$ is the component of $\Delta\boldsymbol{V}_1$ parallel to $\boldsymbol{V}_0$, b_1 is the impact parameter, and $b_{\rm max}$ is the largest impact parameter. (Hereafter $\parallel$ and $\perp$ mean the components parallel and perpendicular to $\boldsymbol{V}_0$, respectively.) Note that we use b and θ as integration variables, which means we chose a circle with the center at the center of coordinate in figure 6 as the region over which we integrate the encounters. By doing so, we made the integration region symmetric for two bodies.

For one encounter, from the momentum conservation, we have

$$M\Delta\boldsymbol{V}_{1\parallel} + M\Delta\boldsymbol{V}_{2\parallel} + m\Delta\boldsymbol{V}_{m\parallel} = 0. \tag{10}$$

Here, m is the mass of a background particle and $\Delta\boldsymbol{V}_m$ is its velocity change. Figure 8 shows the view of the two massive particles and one background particle, on the plane perpendicular to the direction of the motion of massive particles. Since the configuration is symmetric for two massive particles, the dynamical friction on two particles,

after integration in equation (9) is performed, must be equal. Thus, using equation (10), we can replace $\Delta \boldsymbol{V}_1$ in the right-hand side of equation (9) as

$$\Delta \boldsymbol{V}_{1\parallel} = -\frac{m}{2M}\Delta \boldsymbol{V}_{m\parallel}. \tag{11}$$

In the following, we derive the formula for $\Delta \boldsymbol{V}_{m\parallel}$ using impulse approximation. It is expressed as

$$\left|\frac{\Delta \boldsymbol{V}_{m\parallel}}{\boldsymbol{V}_0}\right| = 1 - \cos\psi, \tag{12}$$

where ψ is the deflection angle of the background particle and is expressed as

$$\psi = \left|\frac{\Delta \boldsymbol{V}_{m\perp}}{\boldsymbol{V}_0}\right|. \tag{13}$$

We can calculate $\Delta \boldsymbol{V}_{m\perp}$ using the impulse approximation and by linearly adding the contribution of two massive bodies, $\Delta \boldsymbol{V}_{m1}$ and $\Delta \boldsymbol{V}_{m2}$, as

$$\Delta \boldsymbol{V}_{m\perp} = \Delta \boldsymbol{V}_{m1\perp} + \Delta \boldsymbol{V}_{m2\perp}, \tag{14}$$

$$\Delta \boldsymbol{V}_{m1\perp} = \frac{2G(M+m)}{V_0}\frac{b_1}{b_1^2+\epsilon^2}\hat{\boldsymbol{b}}_1, \tag{15}$$

$$\Delta \boldsymbol{V}_{m2\perp} = \frac{2G(M+m)}{V_0}\frac{b_2}{b_2^2+\epsilon^2}\hat{\boldsymbol{b}}_2, \tag{16}$$

where ϵ is the softening length and $\hat{\boldsymbol{b}}_1$ and $\hat{\boldsymbol{b}}_2$ are the unit vectors in the directions from m to S_1 and S_2 on xy-plane.

Using these formulae, we numerically calculated the dynamical friction on S_1 as a function of the distance between two massive particles d. Figure 9 shows the enhancement β, defined as the increase of the dynamical friction relative to the dynamical friction of single particle moving alone, as the function of the separation d. Here, d_0 is defined as follows:

$$d_0 \equiv \frac{MG}{V_0^2}. \tag{17}$$

We adopt $b_{\max}/d_0 = 100$ and $\epsilon/d_0 = 5.0$. From figure 9, we can see that the increase of the dynamical friction is significant, even when two particles are far away (more than 10 times the softening length).

From this result, we estimated the enhancement of the dynamical friction on the satellite due to the escaped particles. The enhancement factor α is calculated as

$$\alpha = \frac{1}{M_{\rm s}}\int_0^{R_{\rm s}} dr \frac{dm_{\rm e}}{dr}\beta(r), \tag{18}$$

where $m_{\rm e}$ is the total mass of escaped particles within radius r from the center of mass of the satellite and $\beta(r)$ is the value of β at distance r. Note that we made many approximations. First, we approximate the effect of particles at distance r in all directions by that of one particle in the plane perpendicular to the direction of motion. Second, we assume the linear relationship between the mass of the other particle and the enhancement of the dynamical friction. Third, we assume that the effect of multiple particles in different positions can be linearly added.

In figure 10 we plot the value of α at each time step in our simulation. The strength of enhancement changes synchronously with the change of the distance of the satellite from the center of the parent galaxy. The value α is small when the distance is small, *i.e.* near the pericenter, while it is large when the distance is large, *i.e.* near the apocenter.

The effect of this enhancement on the total energy change is shown in figure 6. The difference between the dotted curve and the dash-dotted one corresponds to the enhancement effect, which we call "indirect force". In figure 6, it is shown that the effect of the indirect force is comparable to that of the direct force from escapers. By taking account of the indirect effect, we can explain the change of the total energy quite well.

We performed the semianalytic orbital integration using the dynamical friction enhanced by this parameter α. We also took into account the direct effect of escapers which we discussed in the previous section. Figure 11 shows the result. The agreement between the N-body simulation and the semianalytic integration is excellent. Figures 12 and 13 show the same comparisons for simulations from different initial orbits for the satellite. In both cases, the agreement between our improved treatment and the simulation result is quite good.

5. Summary and Discussions

5.1. Summary

We studied the orbital decay of a satellite galaxy, using a fully self-consistent N-body simulation in which both the satellite and its parent galaxy are expressed by N-body models. We found that the pure dynamical friction, estimated using Chandrasekhar's formula with the correct treatment of Coulomb logarithm of the form proposed by H03, underestimates the drag force by around 20%, at least for the cases we studied.

This rather large discrepancy is due to the effect of particles which are stripped out of the satellite by the tidal field of the parent galaxy. They induce additional drag forces through two mechanisms. The first one is the direct force, which escaped particles exert on the body of the satellite. The particles ejected outward are accelerated by the tidal torque of the satellite, and the satellite loses the energy and angular momentum through the back reaction. The second mechanism is the indirect enhancement of the dynamical friction by particles which are not bound but still in the orbits close to the orbit of the satellite. We found these two mechanisms have comparable contributions and the combined effect quantitatively agrees with the discrepancy between the result of the N-body simulation and the model calculation using pure dynamical friction.

5.2. Comparison with previous works

Jiang and Binney (2000) compared the result of a fully self-consistent N-body simulation and a semianalytic model, for the orbital decay of a satellite galaxy. In their simulation, both the parent galaxy and the satellite were expressed as N-body systems, in the same way as in our work. In the analytic model they used, the orbital evolu-

tion was due to dynamical friction on the bound mass of the satellite, and a simple model was used to evaluate the mass loss due to tidal stripping.

In their work, the orbital evolution obtained with the semianalytic model was faster than that obtained with the N-body simulation. This result is the opposite to what we obtained with our first model, in which we consider only the dynamical friction on the bound mass of the satellite. In other words, the analytical estimate of the effect of dynamical friction in our model was too small, while that in Jiang and Binney (2000) was too large.

The reason of this discrepancy is simple. When applying the Chandrasekhar's dynamical friction formula, we used the variable Coulomb logarithm following H03, while Jiang and Binney (2000) used the constant Coulomb logarithm, which overestimates the dynamical friction. Velazquez & White (1999) also compared N-body simulation and model calculation using dynamical friction formula. They obtained good agreement, but that agreement was achieved by using the Coulomb logarithm as a fitting parameter. H03 argued that the use of the variable Coulomb logarithm would resolve the discrepancy between the N-body simulation and the semianalytic model, without the need for fitting parameter since Coulomb logarithm is calculated from the size of the satellite and its distance to the center of the parent galaxy.

We found that the variable Coulomb logarithm of H03 alone would *underestimate* the total drag on a live (self-consistent) satellite, when the tidal mass loss is significant. A physically meaningful model need to incorporate the effect of escaped particles in some way.

5.3. CDM substructures

In this paper we considered an idealized model of a spherical satellite galaxy orbiting in a spherical parent galaxy. In the CDM cosmology, most of the mass of a galaxy is in the CDM halo and satellite galaxies, at least at their formation times, are in massive CDM subhalos. Recent N-body simulation of the formation and evolution of CDM halos (Kravtsov et al. 2004; Kase et al. 2006) showed that most of subhalos lose 90% or more of their initial mass after they become bound to the main halo through tidal mass loss. Thus, the mass loss they experience is typically much bigger than the mass loss occurring to our model satellite. We can infer that the effect of mass loss on the orbital evolution of CDM substructures or satellite galaxies is even bigger than what we found.

5.4. Star Clusters

The orbits of star clusters evolve through dynamical friction. Whether or not the effect of escaped particles are important is not clear. Both the timescale of the orbital evolution and that of mass loss are significantly longer than the orbital timescale. Thus, we need more careful analysis to study these effects. In the case of very young clusters born close to the galactic center (Figer et al. 1999; McCrady, Gilbert and Graham 2003), we can expect the effect of the escapers to be significant, since the ratio between the cluster mass and the relevant mass of the parent galaxy (mass inside the location of the cluster) is not too different from that ratio between the satellite and the parent galaxy in our model. For most of the numerical studies of star clusters, the pure dynamical friction formula has been used (e.g., Portegies Zwart and McMillan 2002; Baumgardt and Makino 2003; Gürkan and Rasio 2005) These works might have significantly overestimated the timescale of orbital evolution. We will study these cases in the forthcoming paper.

The authors thanks Hiroyuki Kase, Keigo Nitadori and Masaki Iwasawa for helpful discussions, Piet Hut, J. E. Taylor, and G. Bertin for useful comments on the manuscript, and Shunsuke Hozumi for detailed comments which helped us to significantly improve the presentation of the paper. This research is partially supported by the Special Coordination Fund for Promoting Science and Technology (GRAPE-DR project), Ministry of Education, Culture, Sports, Science and Technology, Japan.

References

Barnes, J., & Hut, P. 1986, Nature, 324, 446
Baumgardt, H., & Makino, J. 2003, MNRAS, 340, 227
Binney, J., & Tremaine S. 1987, Galactic Dynamics (Princeton: Princeton Univ. Press), 424
Bullock, J. S., & Johnston, K.V. 2005, ApJ, 635, 931
Chandrasekhar, S. 1943, ApJ, 97, 255
Figer, D. F., Kim, S. S., Morris, M., Serabyn, E., Rich, R. M., & McLean, I. S. 1999, ApJ, 525, 750
Fukushige, T., Makino, J., & Kawai, A. 2005, PASJ, 57, 1009
Funato, Y., Makino, J., & Ebisuzaki, T. 1993, PASJ, 45, 289
Gürkan, M. A., & Rasio, F. A. 2005, ApJ, 628, 236
Hashimoto, Y., Funato, Y., & Makino, J. 2003, ApJ, 582, 196
Heggie, D.C., & Mathieu, R.D. 1986, in The Use of Supercomputers in Stellar Dynamics, ed. P. Hut, and S. McMillan (Lecture Notes in Physics 267; Berlin: Springer), 233
Helmi, A., White, S. D. M., de Zeeuw, P. T. & Zhao, H. 1999, Nature 402, 53
Ibata, R. A., & Lewis, G. F. 1998, ApJ, 500, 575
Jiang, I.-G., & Binney, J. 2000, MNRAS, 314, 468
Johnston, K. V., Spergel, D. N., & Hernquist, L. 1995, ApJ, 451, 598
Kase, H., Funato, Y., & Makino, J. 2005, in preparation
Kravtsov, A. V., Gnedin, O. Y., Klypin, A. A. 2004, ApJ, 609, 482
Makino, J. 1991, PASJ, 43, 621
Makino, J. 2004, PASJ, 56, 521
McCrady, N., Gilbert, A. M., & Graham, J. R. 2003, ApJ, 596, 240
Murai, T., & Fujimoto, M. 1980, PASJ, 32, 581
Portegies Zwart, S. F., & McMillan, S. L. W. 2002, ApJ, 576, 899
Portegies Zwart, S. F., Baumgardt, H., Hut, P., Makino, J., & McMillan, S. L. W, 2004, Nature, 428, 724
Spitzer, L. 1987, Dynamical evolution of globular clusters (Princeton: Princeton Univ. Press), 119
Taylor, J. E., & Babul, A. 2001, ApJ, 559, 716
van den Bosch, F. C., Lewis, G. F., Lake, G., & Stadel, J. 1999, ApJ, 515, 50
Velazquez, H., & White, S. D. M. 1999, MNRAS, 304, 254

White, S. D. M. 1976, MNRAS, 174, 467
Zentner, A. R., & Bullock, J. S. 2003, ApJ, 598, 49

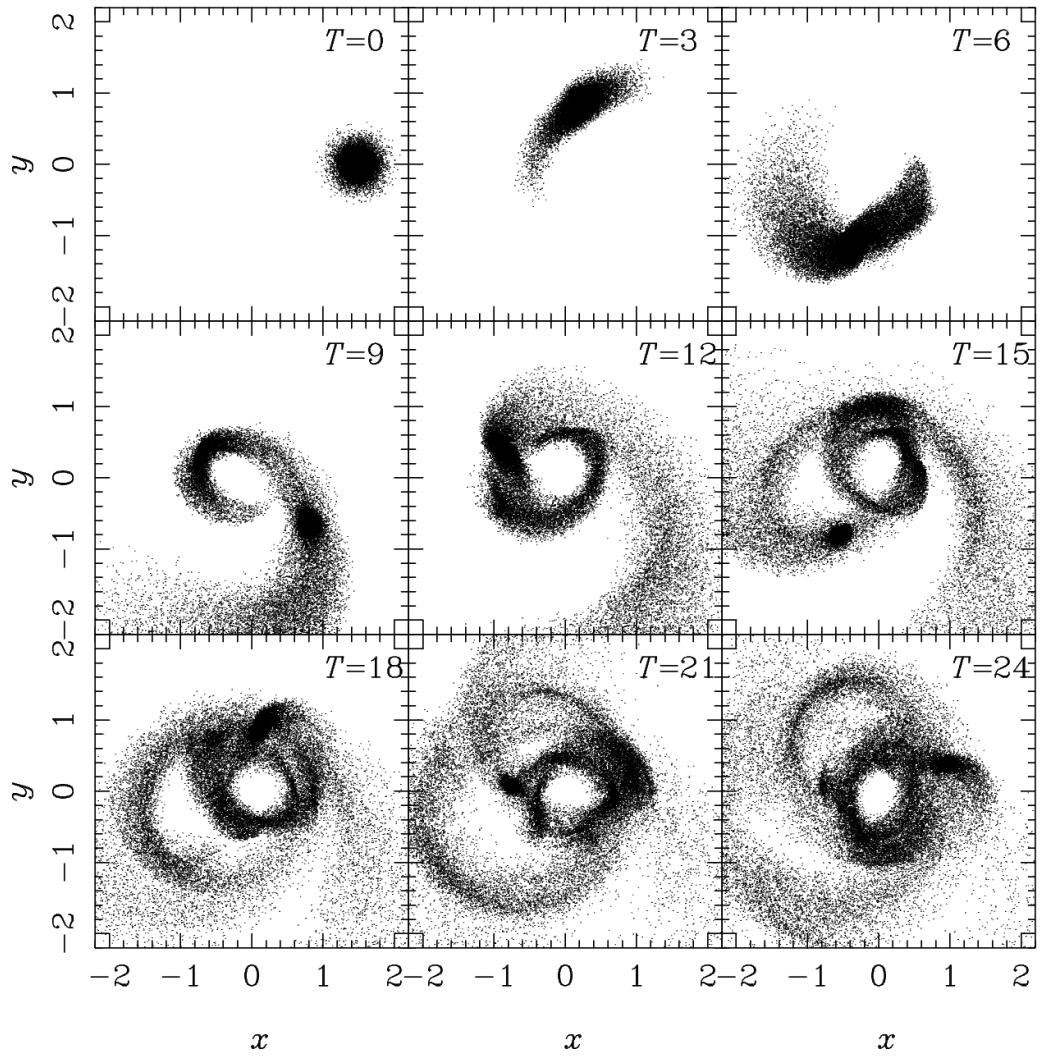

Fig. 1. Snapshots of the satellite particles projected onto the xy-plane.

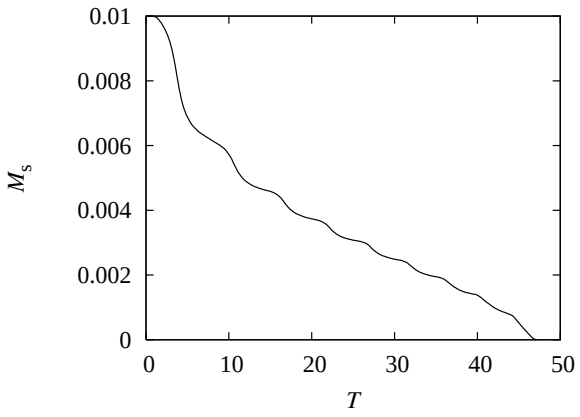

Fig. 2. Bound mass of the satellite M_s plotted as a function of time T.

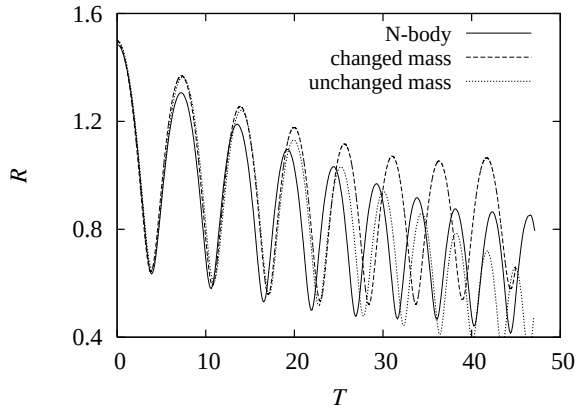

Fig. 3. The distance of the satellite from the center of the parent galaxy plotted as a function of time. Solid curve shows the result of the N-body simulation. Dashed and dotted curves show that of semianalytic calculations, in which the mass and size of the satellite is changed (*dashed curve*) and unchanged (*dotted curve*).

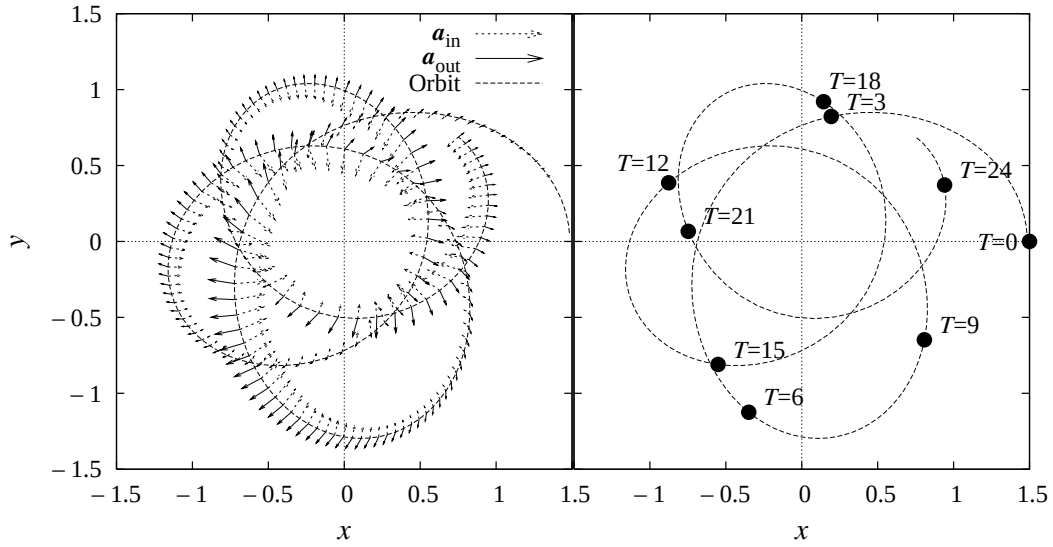

Fig. 4. The direction and strength of the direct effect $\boldsymbol{a}_{\rm di}$, along with the orbit of the satellite. The left panel shows contributions from particles outside the radius of the satellite and that from inside as $\boldsymbol{a}_{\rm out}$ and $\boldsymbol{a}_{\rm in}$ (The sum of these two terms gives $\boldsymbol{a}_{\rm di}$). The length of the arrow is 20 times the absolute value of the acceleration. The right panel shows the orbit of the satellite, with the time shown for filled circles.

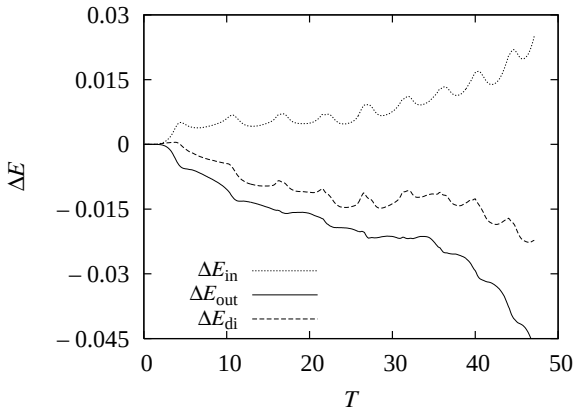

Fig. 5. The change of the orbital binding energy due to the direct effect of escaped particles. Dotted, solid and dashed curves indicate the effect of particles inside, particles outside and total effect, respectively.

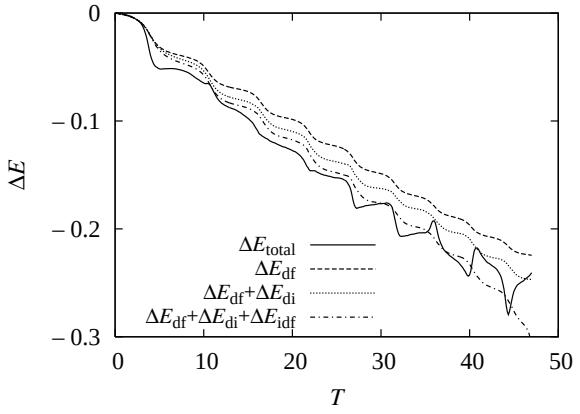

Fig. 6. The evolution of the orbital energy of the satellite plotted as the function of time. Solid curve shows the change of the orbital energy $\Delta E_{\rm total}$ obtained by the N-body simulation. Dashed curve shows the estimated energy change $\Delta E_{\rm df}$ due to the dynamical friction. Dotted curve shows the energy change due to the dynamical friction plus the direct effect of escaped particles $\Delta E_{\rm df} + \Delta E_{\rm di}$. Dash-dotted curve shows that due to the dynamical friction and the direct and indirect forces from escaped particles $\Delta E_{\rm df} + \Delta E_{\rm di} + \Delta E_{\rm idf}$.

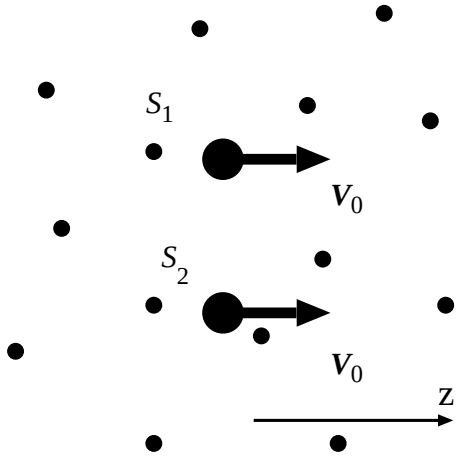

Fig. 7. Two massive objects moving in a uniform distribution of background field particles.

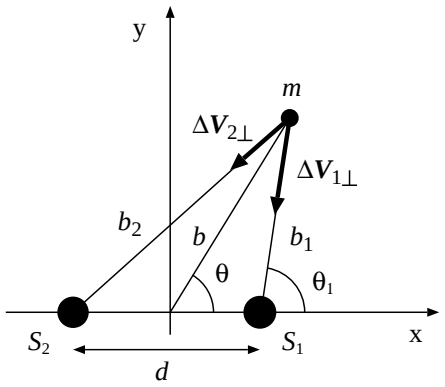

Fig. 8. View of two massive objects and one background particle on the plane perpendicular to the direction of the motion of massive particles.

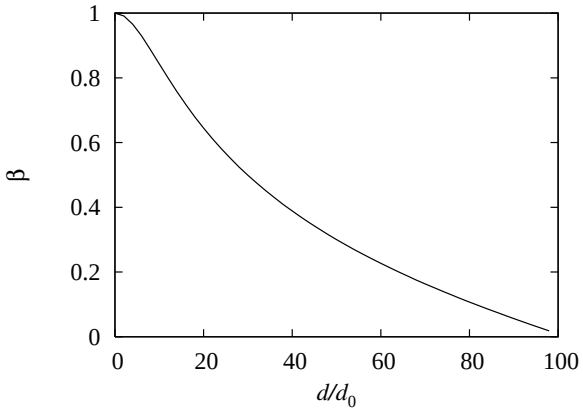

Fig. 9. The relative increase of the dynamical friction β as a function of the normalized distance between two objects.

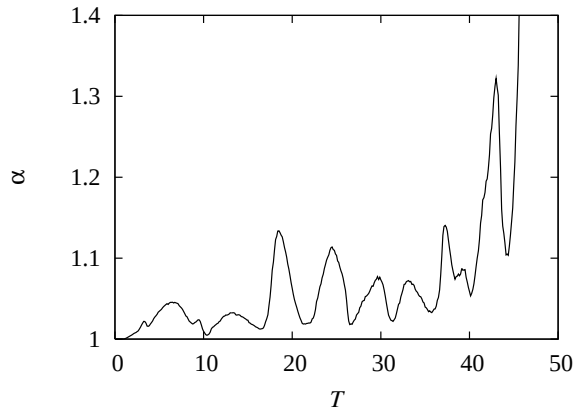

Fig. 10. The enhancement factor α as a function of time.

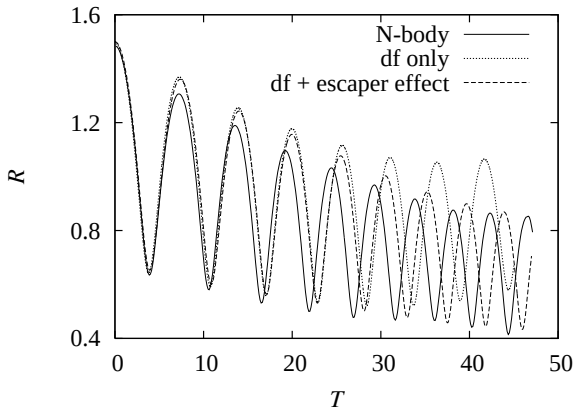

Fig. 11. Same as Fig. 3, but the result of semianalytic integration using only the pure dynamical friction is shown in the dotted curve and that with dynamical friction and both the direct and indirect effect of escapers is shown in the dashed curve.

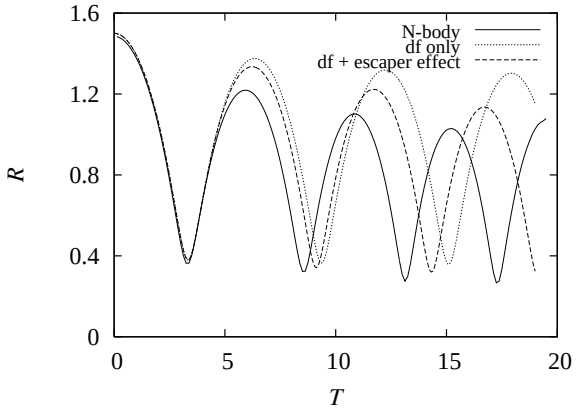

Fig. 12. Same as Fig. 11 but the initial velocity of the satellite is 0.326. In this calculation, the satellite was disrupted at around $T = 20$

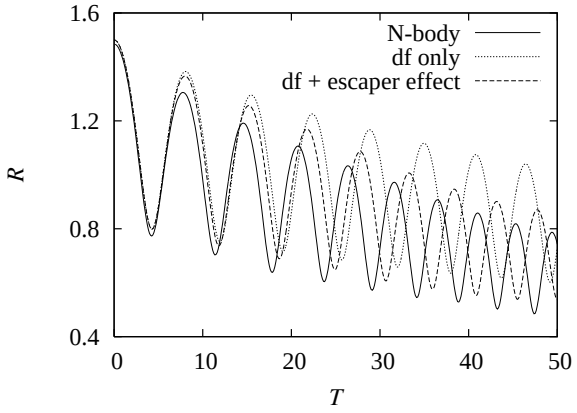

Fig. 13. Same as Fig. 11 but the initial velocity of the satellite is 0.5.